Available online at www.sciencedirect.com
ScienceDirect
Polymer 47 (2006) 7881–7888
polymer
www.elsevier.com/locate/polymer

New hyperbranched polymers containing second-order nonlinear optical chromophores: Synthesis and nonlinear optical characterization

Zhichao Zhu [a], Zhong'an Li [a], Yong Tan [a], Zhen Li [a,*], Qianqian Li [a], Qi Zeng [a], Cheng Ye [b], Jingui Qin [a,*]

[a] *Hubei Key Lab on Organic and Polymeric Opto-Electronic Materials, Department of Chemistry, Wuhan University, Wuhan 430072, PR China*
[b] *Organic Solids Laboratories, Institute of Chemistry, The Chinese Academy of Sciences, Beijing 100080, PR China*

Received 13 July 2006; received in revised form 4 September 2006; accepted 24 September 2006
Available online 10 October 2006

Abstract

Three hyperbranched polymers (**P1**–**P3**) containing second-order nonlinear optical chromophores were synthesized by copolymerization of aromatic dialdehydes (carbazole, triphenylamine or benzene moieties) with sulfonyl-based chromophores attached with three active methylene groups, from "$A_2 + B_3$" approach based on simple Knoevenagel reaction. For comparison, their corresponding linear analogue polymers (**P4**–**P6**) were prepared. All the polymers are soluble in common organic solvents, and exhibit good thermal stability. The tested NLO properties of the hyperbranched polymers are better than their corresponding linear polymers, due to the three-dimensional spatial separation of the chromophores in the obtained hyperbranched polymeric structures.

Keywords: Hyperbranched polymers; Synthesis; Nonlinear optics

1. Introduction

Due to their advantages such as large nonlinearity, good processability, ultra-fast response time and superior chemical flexibility, organic and polymeric nonlinear optical (NLO) materials are considered as viable alternatives to conventional inorganic crystalline materials, in which lithium niobate is the typical delegate [1]. To exhibit electro-optical (EO) effect, the active moieties, NLO chromophores should be generally poled under an electric field, to form a highly ordered noncentrosymmetric alignment. However, chromophores with high first-order hyperpolarizability usually have large dipole moments, which directly lead to the strong intermolecular dipole–dipole interactions in the polymeric system, making the poling-induced noncentrosymmetric alignment a daunting task [2]. This reason accounts for the fact that the NLO properties of the polymers are only enhanced several times even if the $\mu\beta$ values of chromophores have been improved by up to 250 folds, thanks to the great efforts of scientists in the past decades. Thus, it is still a big challenge in this area to efficiently translate large molecular first hyperpolarizability (β) value into high macroscopic second-harmonic generation (SHG) coefficient [3].

Much work has been done to tackle this problem. And recent theoretical analyses suggest that optimization of molecular shape can minimize this intermolecular electrostatic interaction and enhance the poling efficiency to some degree, bringing about a boost in the maximum realizable EO activity, with spherical shape, proposed by Dalton et al., being the most ideal conformation [4]. This is further proved by Jen et al. in the NLO dendrimers and polyimides containing dendronized chromophores in the side chains [5]. Similar to dendrimers, hyperbranched polymers possess many unusual properties in comparison with conventional linear polymers. Especially, both of them are globular macromolecules, well suited for the ideal shape modification of NLO chromophores. Also, the three-dimensional spatial separation of the chromophores

* Corresponding authors. Tel./fax: +86 27 68756757 (Z.L.).
E-mail address: lizhen@whu.edu.cn (Z. Li).

0032-3861/$ - see front matter © 2006 Elsevier Ltd. All rights reserved.
doi:10.1016/j.polymer.2006.09.047

endows the polymers with favorable site-isolation effect, and their void-rich topological structure helps to minimize optical loss in the NLO process [6–8].

To deepen the exploration of the fundamental architectural design parameters and develop NLO hyperbranched polymers, based partly on our previous research [9], in this work, we designed and synthesized three NLO hyperbranched polymers (**P1**–**P3**) (Scheme 1), in which the common azo chromophores with sulfonyl moieties as the acceptor were used as the NLO active units. Due to the synthetic flexibility of sulfonyl chromophores, we also prepared the corresponding linear analogues (**P4**–**P6**). The hyperbranched polymers are macroscopically processable, thermolytically resistant, and morphologically stable, and the tested NLO values of the hyperbranched polymers are better than their analogue linear polymers, due to the special structure and several advantages of hyperbranched polymers. Herein, we would like to report the syntheses, characterization and NLO properties of these polymers.

2. Experimental

2.1. Materials

Tetrahydrofuran (THF) was dried over and distilled from K–Na alloy under an atmosphere of dry nitrogen. *N*,*N*-Dimethylformamide (DMF) was dried over and distilled from CaH_2 under an atmosphere of dry nitrogen. $POCl_3$ was freshly distilled before use. *N*,*N*-Di-(2-hydroxyethyl)amine (**1**) was bought from Fluka. Triphenylamine was purchased from Alfa Aesar. *p*-(Hydroxyethylsulfonyl)aniline (**2**) and *p*-(ethylsulfonyl)aniline (**3**) were prepared according to the literature [10]. *N*-Hexylcarbazole (**8**) was synthesized as reported previously [11]. Bis-(4-formylphenyl)phenyl amine (**10**) was obtained by the method reported in the literature [12]. All other reagents and solvents were used as received without further purification.

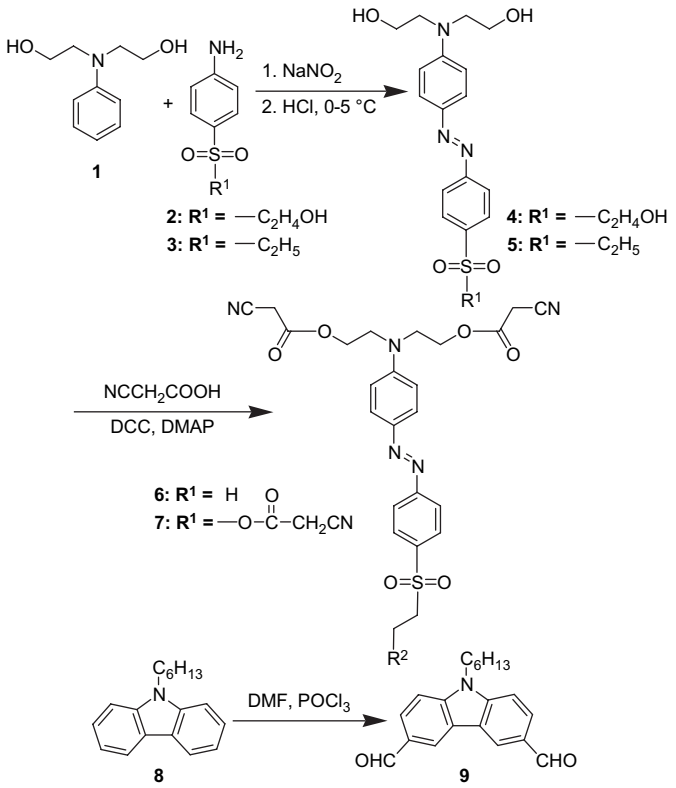

Scheme 1.

2.2. Instrumentation

^{1}H NMR and ^{13}C NMR spectroscopic study was conducted with a Varian Mercury300 spectrometer using tetramethylsilane (TMS; $\delta = 0$ ppm) as internal standard. The Fourier transform infrared (FTIR) spectra were recorded on a Perkin-Elmer-2 spectrometer in the region of 4000–400 cm^{-1}. UV–vis spectra were obtained using a Shimadzu 160A spectrometer. Mass spectral analysis was performed on API 200 LC/MS system or with a VJ-ZAB-3F-Mass spectrometer. Elementary analysis was taken on a Vario EL III elementary analysis instrument. Gel permeation chromatography (GPC) was used to determine the molecular weights of polymers. GPC analysis was performed on an Agilent 1100 series HPLC system and a G1362A refractive index detector. Polystyrene standards were used as calibration standards for GPC. THF was used as an eluent and the flow rate was 1.0 mL/min or GPC was conducted on a Waters HPLC system equipped with a 2690D separation module and a 2410 refractive index detector, with DMF as an eluent and the flow rate 1.0 mL/min. Thermal analysis was performed on Netzsch STA449C thermal analyzer at a heating rate of 20 °C/min in argon at a flow rate of 50 cm^3/min for thermogravimetric analysis (TGA). The thermal transitions of the polymers were investigated using a Netzsch differential scanning calorimeter DSC200PC under nitrogen at a scanning rate of 10 °C/min. The thermometer for measurement of the melting point was uncorrected. The thickness of the films was measured with an Ambios Technology XP-2 profilometer.

2.3. Synthesis of *4*

Compound **4** was prepared similarly according to the method described in the literature. *p*-(Hydroxyethylsulfonyl)-aniline (**2**) (0.40 g, 1.94 mmol), sodium nitrite (0.14 g, 2 mmol) and water (2 mL) were placed in a flask, then 18% (wt%) hydrochloride acid (4.4 mL) was added slowly at 0 °C. After stirred for 30 min below 2 °C, the mixture was filtered to give a pink solution. To this solution was added dropwise the solution of *N*-di-(2-hydroxyethyl)amine (**1**) (0.37 g, 2 mmol) in ethanol (2.5 mL), and the resultant mixture was agitated in an ice bath for 1.5 h. The crude product was precipitated out by neutralizing the reaction mixture with the aqueous solution of sodium bicarbonate, and was further purified by recrystallization from acetone to afford an orange crystalline solid (0.55 g, 70%). Mp: 158–161 °C. ^{1}H NMR (acetone-d_6) δ (ppm): 3.34 (t, $J = 5.7$ Hz, 2H, $-SO_2CH_2-$), 3.60 (t, $J = 5.1$ Hz, 4H, $-NCH_2CH_2$), 3.70 (t, $J = 5.1$ Hz, 4H, $-O-CH_2CH_2-$), 4.07 (t, $J = 6.0$ Hz, 2H, $-CH_2CH_2-O-$),

6.83 (d, $J = 9.6$ Hz, 2H, ArH), 7.75 (d, $J = 8.7$ Hz, 2H, ArH), 7.86 (d, $J = 8.7$ Hz, 2H, ArH), 7.94 (d, $J = 9.0$ Hz, 2H, ArH). IR (thin film) ν (cm^{-1}): 3352 (−OH), 1135 ($-SO_2-$). UV−vis (THF, 2.5×10^{-5} mol/L): λ_{max} (nm): 446. MS (EI) *m/z* [M^+]: 393.7, calcd 393.1.

2.4. Synthesis of **5**

Compound **5** was obtained from the similar procedure as that for **4**, except that *p*-(ethylsulfonyl)aniline was used instead of *p*-(hydroxyethylsulfonyl)aniline. Yield: 96%. Mp: 129−130 °C. ^{1}H NMR (acetone-d_6) δ (ppm): 1.30 (t, $J = 7.5$ Hz, 3H, $-CH_3$), 3.17 (q, 2H, $-SO_2CH_2-$), 3.75 (t, $J = 5.1$ Hz, 4H, $-NCH_2CH_2$), 3.97 (s, br, 4H, $-O-CH_2CH_2-$), 6.81 (d, $J = 9.0$ Hz, 2H, ArH), 7.91 (d, $J = 8.7$ Hz, 2H, ArH), 7.98 (q, 4H, ArH). IR (thin film) ν (cm^{-1}): 3346 (−OH), 1131 ($-SO_2-$). UV−vis (THF, 2.5×10^{-5} mol/L): λ_{max}: 448 nm.

2.5. Synthesis of chromophores **6** and **7**

The general synthetic procedure for these two compounds was similar, and that of **7** was described in detail as an example. Compound **4** (0.20 g, 0.50 mmol), cyanoacetic acid (0.29 g, 3.0 mmol) and 4-(*N*,*N*-dimethyl)aminopyridine (0.10 g, 0.81 mmol) were dissolved in dry DMF (15 mL), then dicyclohexylcarbodiimine (1.90 g, 0.90 mmol) was added quickly. The resultant mixture was stirred at room temperature for 42 h. The precipitate was filtered, and the filtrate was poured into saturated salt solution. The orange solid was collected, washed subsequently with 0.5 M hydrochloride acid, diluted aqueous solution of sodium bicarbonate, and water. The crude product was further purified by column chromatography on silica gel for two times. First, the mixture of petroleum and ethyl acetate (1:3, v/v) was used as eluent. And in the second run, the eluent was dichloromethane plus a little amount of ethyl acetate (about 5%). A pure orange product was yielded (0.14 g, 47%). Mp: 53−55 °C. ^{1}H NMR (acetone-d_6) δ (ppm): 3.66 (s, 2H, $-OCOCH_2CN$), 3.74 (t, $J = 6.0$ Hz, 2H, $-SO_2CH_2-$), 3.85 (s, 4H, $-OCOCH_2CN$), 3.97 (t, $J = 6.0$ Hz, 4H, $-NCH_2CH_2$), 4.49 (t, $J = 6.0$ Hz, 4H, $-O-CH_2CH_2-$), 4.56 (t, $J = 5.7$ Hz, 2H, $-CH_2CH_2-OCO-$), 7.09 (d, $J = 8.7$ Hz, 2H, ArH), 7.94 (d, $J = 9.0$ Hz, 2H, ArH), 8.05 (d, $J = 8.7$ Hz, 2H, ArH), 8.12 (d, $J = 8.7$ Hz, 2H, ArH). ^{13}C NMR (acetone-d_6) δ (ppm): 24.1, 24.3, 49.5, 54.5, 59.7, 63.5, 112.3, 113.7, 114.1, 122.9, 126.0, 129.6, 139.9, 144.2, 151.6, 156.4, 163.8, 164.3. IR (thin film) ν (cm^{-1}): 2264 (CN), 1742 (C=O), 1123 ($-SO_2-$). Anal. Calcd for $C_{27}H_{26}N_6O_8S$: C, 54.54; H, 4.41; N, 14.13; S, 5.39. Found: C, 54.51; H, 4.51; N, 14.04; S, 5.11. UV−vis (THF, 2.5×10^{-5} mol/L): λ_{max} (nm): 429. MS (FAB) *m/z* [M^+]: 595.0, calcd 594.2.

Compound **6**: for the preparation of this compound, THF was used instead of DMF, and the crude product was purified by column chromatography on silica gel using ethyl acetate/petroleum ether (3/1) as eluent. Yield: 79.6%. Mp: 50−51 °C. ^{1}H NMR ($CDCl_3$) δ (ppm): 1.15 (t, 3H, $-CH_3$), 3.18 (q, 2H, $-SO_2CH_2-$), 3.45 (s, 4H,$-CH_2CN$), 3.86 (t, 4H, $-NCH_2CH_2$), 4.48 (t, $J = 6.0$ Hz, 4H, $-O-CH_2CH_2-$), 6.87 (d, $J = 8.7$ Hz, 2H, ArH), 7.96 (d, $J = 9.3$ Hz, 2H, ArH), 7.99 (s, br, 4H, ArH). IR (thin film) ν (cm^{-1}): 2264 (CN), 1750 (C=O), 1129 ($-SO_2-$). UV−vis (THF, 2.5×10^{-5} mol/L): λ_{max} (nm): 426. MS (EI) *m/z* [M^+]: 512.1, calcd 511.2.

2.6. Synthesis of **9**

To *N*,*N*-dimethylformamide (DMF) (16 mL, 0.20 mol) at 0 °C, was added dropwise phosphorus oxychloride (18.5 mL, 0.20 mol). The solution was then warmed up to room temperature, and compound **8** (5.03 g, 20 mmol) was added. The resultant mixture was heated to 80 °C and stirred at this temperature for 16 h. After reaction, the mixture was poured into ice water (300 ml), and extracted with chloroform for several times. Removal of chloroform gave the crude product with deep color, which was purified on a silica column using hexane/ethyl acetate (7:3 by volume) as eluent (2.46 g, 40%). Mp: 130 °C. ^{1}H NMR ($CDCl_3$) δ (ppm): 0.87 (t, $J = 6.9$ Hz, 3H, $-CH_3$), 1.43−1.25 (m, 6H, $-CH_2-$), 1.92 (m, 2H, $-CH_2CH_2$), 4.39 (t, $J = 7.2$ Hz, 2H, $-NCH_2CH_2$), 7.57 (d, $J = 8.4$ Hz, 2H, ArH), 8.11 (d, $J = 7.8$ Hz, 2H, ArH), 8.68 (s, 2H, ArH), 10.14 (s, 2H, −CHO). IR (thin film) ν (cm^{-1}): 1685 (C=O), 1625, 1593 (carbazole ring).

2.7. Synthesis of **P1−P6**

The general procedure was alike for the preparation of **P1−P6**, and the synthesis of **P1** was given as an example.

A 50-mL Schlenk tube was charged with **7** (0.13 g, 0.22 mmol), **9** (0.10 g, 0.33 mmol), and hexahydropyridine (0.07 mL) as a basic catalyst in DMF (3.5 mL) with a stirring bar under the atmosphere of dry nitrogen. The reaction mixture was stirred at 110 °C for about 2 h, then poured into methanol (250 mL) after cooled to room temperature. The orange precipitate was collected and purified by several reprecipitations from THF to methanol. The product was dried under vacuum (0.17 g, 73.9%). $M_w = 5000$, $M_w/M_n = 1.20$ (GPC, polystyrene calibration). ^{1}H NMR (DMSO-d_6) δ (ppm): 0.73 ($-CH_3$), 1.10−1.17 ($-NCH_2CH_2CH_2CH_2CH_2$), 1.49 ($-NCH_2CH_2-$), 3.42 ($-SO_2CH_2-$), 3.56 ($-NCH_2CH_2-$), 3.99 ($-O-CH_2CH_2-$), ($-NCH_2-$), 4.56 ($-CH_2CH_2-O-$), 7.17−7.35 (ArH), 7.53−7.84 (ArH), 7.98 (−CH=CH−). IR (thin film) ν (cm^{-1}): 2214 (CN), 1722 (C=O), 1583 (C=C), 1132 ($-SO_2-$). UV−vis (THF, 0.02 mg/mL): λ_{max} (nm): 407.

P2: orange powder, 54.5%. $M_w = 4200$, $M_w/M_n = 1.83$ (GPC, polystyrene calibration). ^{1}H NMR (DMSO-d_6) δ (ppm): 3.51 ($-SO_2CH_2-$), 3.59 ($-NCH_2CH_2-$), 3.94 ($-O-CH_2CH_2-$), 4.49 ($-CH_2CH_2-O-$), 6.89−7.39 (ArH), 7.82 (ArH), 7.96 (−CH=CH−). IR (thin film) ν (cm^{-1}): 2223 (CN), 1722 (C=O), 1578 (C=C), 1129 ($-SO_2-$). UV−vis (THF, 0.02 mg/mL): λ_{max} (nm): 434.

P3: orange powder, 45.0%. $M_w = 6300$, $M_w/M_n = 1.29$ (GPC, polystyrene calibration). ^{1}H NMR (DMSO-d_6) δ (ppm): 3.55 ($-SO_2CH_2-$), 3.98 ($-NCH_2CH_2-$), 4.54 ($-O-CH_2CH_2-$), 4.88 ($-CH_2CH_2-O-$), 6.86−7.11 (ArH), 7.79−7.89 (ArH), 7.99 (−CH=CH−). IR (thin film) ν (cm^{-1}): 2223

(CN), 1728 (C=O), 1600 (C=C), 1131 (−SO_2−). UV−vis (THF, 0.02 mg/mL): λ_{max} (nm): 432.

P4: orange powder, 26.1%. $M_w = 13{,}000$, $M_w/M_n = 1.18$ (GPC, DMF as eluent, polystyrene calibration). ^{1}H NMR (DMSO-d_6) δ (ppm): 0.76 (−CH_2CH_3−), 1.10 (br, −$NCH_2CH_2CH_2CH_2CH_2CH_3$), 1.58 (−$NCH_2CH_2$−), 3.59 (−$SO_2CH_2$−), 3.87 (−$NCH_2CH_2$−), 4.03 (−$NCH_2$−), 4.59 (−O−$CH_2CH_2$−), 7.21−7.79 (ArH), 7.86 (−CH=CH−). IR (thin film) ν (cm^{-1}): 2223 (CN), 1722 (C=O), 1580 (C=C), 1129 (−SO_2−). UV−vis (THF, 0.02 mg/mL): λ_{max} (nm): 407.

P5: orange powder, 48.2%. $M_w = 5700$, $M_w/M_n = 2.40$ (GPC, polystyrene calibration). ^{1}H NMR (DMSO-d_6) δ (ppm): 1.09 (−CH_2CH_3−), 3.57−3.61 (−SO_2CH_2−), 4.47 (−NCH_2CH_2−), 4.85 (−O−CH_2CH_2−), 7.01−7.12 (ArH), 7.79−7.91 (ArH), 7.94 (−CH=CH−). IR (thin film) ν (cm^{-1}): 2223 (CN), 1719 (C=O), 1578 (C=C), 1129 (−SO_2−). UV−vis (THF, 0.02 mg/mL): λ_{max} (nm): 432.

P6: orange powder, 33%. $M_w = 20{,}000$, $M_w/M_n = 1.07$ (GPC, DMF as eluent, polystyrene calibration). ^{1}H NMR (DMSO-d_6) δ (ppm): 1.11 (−CH_2CH_3−), 3.57−3.61 (−SO_2CH_2−), 4.27 (−NCH_2CH_2−), 4.82 (−O−CH_2CH_2−), 6.93 (ArH), 7.42−7.47, 7.79 (ArH), 7.95 (−CH=CH−). IR (thin film) ν (cm^{-1}): 2206 (CN), 1667 (C=O), 1600 (C=C), 1129 (−SO_2−). UV−vis (DMF, 0.02 mg/mL): λ_{max} (nm): 440.

2.7.1. Film fabrication

The polymers were dissolved in THF (concentration ~2 wt%) or DMF (concentration ~3 wt%), and the solutions were filtered through syringe filters. The polymer solutions were spin coated onto indium-tin oxide (ITO)-coated glass substrates, which were carefully pre-cleaned by DMF, acetone, distilled water, and THF sequentially in ultrasonic bath. Residual solvent was removed by heating the polymer films in a vacuum oven at 40 °C for 2 days.

2.7.2. NLO measurement

The second-order optical nonlinearity of the polymers was determined by in situ SHG experiments using a closed temperature-controlled oven with optical windows and three needle electrodes. The films were kept at 45° to the incident beam and poled inside the oven, with the SHG intensity monitored simultaneously. Poling conditions were as follows: temperature: different for each polymer (Table 1); voltage: 7.5 kV at the needle point; gap distance: 0.8 cm. The SHG measurements were carried out with a Nd:YAG laser operating at a repetition rate of 10 Hz and a pulse width of 8 ns at 1064 nm. A Y-cut quartz crystal was used as reference.

3. Results and discussion

3.1. Synthesis

Compounds **4**−**5** were prepared by the normal azo coupling reactions; it was important to keep the reaction temperature below 2 °C during the experiment to achieve high yields. Compounds **6**−**7** were synthesized by the reaction between the cyanoacetic and the corresponding alcohol, **4** or **5**, and all the reacting compounds and the solvent should be well dried [13].

As shown in Scheme 2, hyperbranched polymers **P1**−**P3** were obtained by the Knoevenagel condensation reactions from "$A_2 + B_3$" approach. The chromophore active moieties were the same (chromophore **7**), while the co-monomers changed from small bulky groups (benzene ring) to larger groups (TPA or CZ moieties). For comparison, the analogue linear polymers (**P4**−**P6**) of **P1**−**P3** were also prepared under the similar conditions (Scheme 3) but chromophore **6** was used instead of chromophore **7**. It is easily seen that chromophores **6** and **7** possess the same donor−π-acceptor structure, and their only difference is the number of the active methylene moieties. This is the special point of sulfonyl-based chromophores as claimed previously, which offers the large synthetic flexibility

Table 1
Polymerization results and characterization data

No.	Yield (%)	M_w[a]	M_w/M_n[a]	λ_{max}[b] (nm)	T_g[c] (°C)	T_d[d] (°C)	T[e] (°C)	l_s[f] (μm)	d_{33}[g] (pm/V)
P1	73.9	5000	1.20	407 (412)	130	246	91	0.43	51.1
P2	54.5	4200	1.83	434 (436)	146	230	126	0.53	44.7
P3	45.0	6300	1.29	432 (439)	134	212	90[h]	0.29[h]	20.6[h]
P4	26.1[i]	13,100[i]	1.18[i]	407 (413)	144	270		0.37	13.4
P5	48.2	5700	2.40	432 (434)	116	255		0.15	20.1
P6	33.0[i]	20,000[i]	1.07[i]	(440)		271			
6	79.6			426 (436)					
7	47.0			429 (437)					

[a] Determined by GPC in THF on the basis of a polystyrene calibration.
[b] The maximum absorption wavelength of polymer solutions in THF, while the maximum absorption wavelength of their diluted solutions in DMF are given in the parentheses.
[c] Glass transition temperature (T_g) of polymers detected by the DSC analyses under nitrogen at a heating rate of 10 °C/min.
[d] The 5% weight loss temperature of polymers detected by the TGA analyses under argon at a heating rate of 20 °C/min.
[e] The best poling temperature.
[f] Film thickness.
[g] Second-harmonic generation (SHG) coefficient.
[h] Tested in the doped PMMA film with the concentration of 50% (w/w).
[i] Determined by GPC in DMF on the basis of a polystyrene calibration.

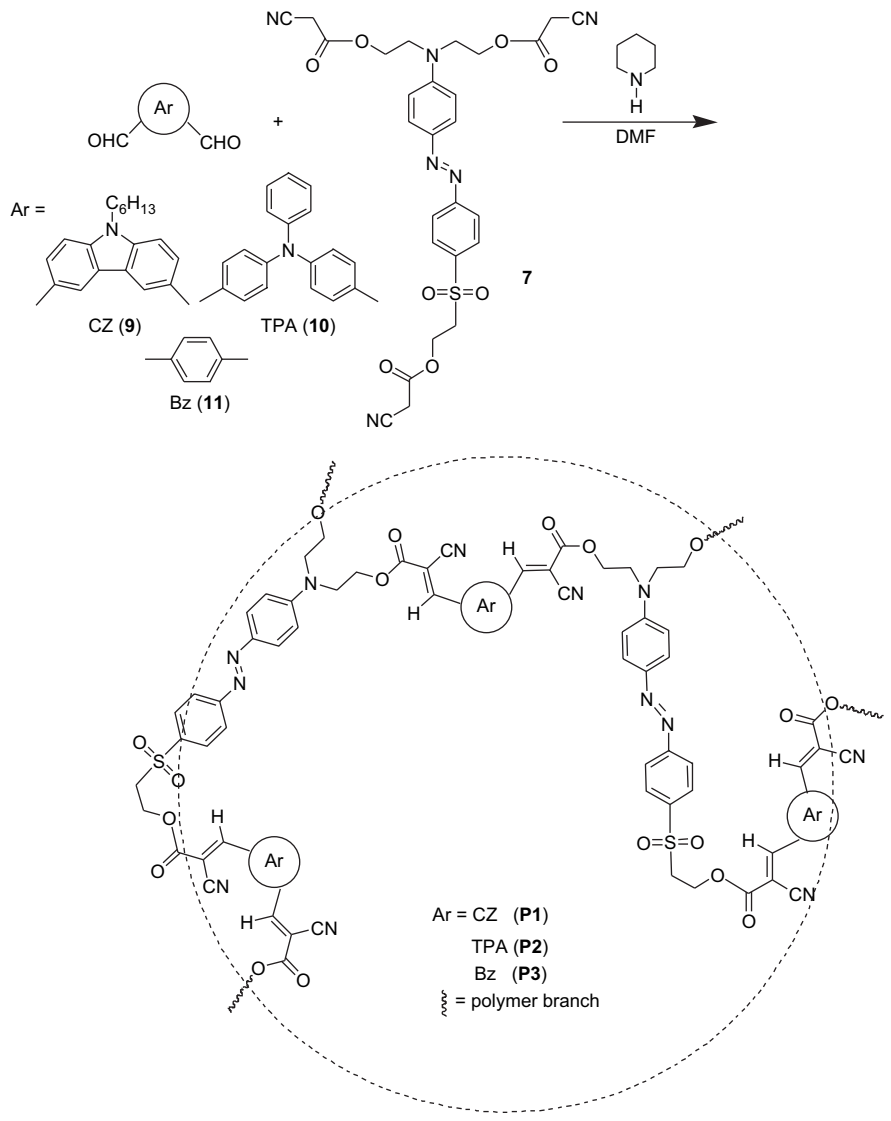

Scheme 2.

[14]. By adjusting the groups linked to the sulfur atoms, we could easily construct linear or hyperbranched polymers from the sulfonyl-based chromophores, and in the resultant polymers, the concentrations of the NLO chromophores in the hyperbranched polymers are only a little lower than in their corresponding analogue linear ones. Another special advantage is that the sulfonyl-based chromophores exhibit good transparency, leading to the wider transparency window [14].

During the polymerization process of hyperbranched polymers, the reactions were monitored by dropping small fractions

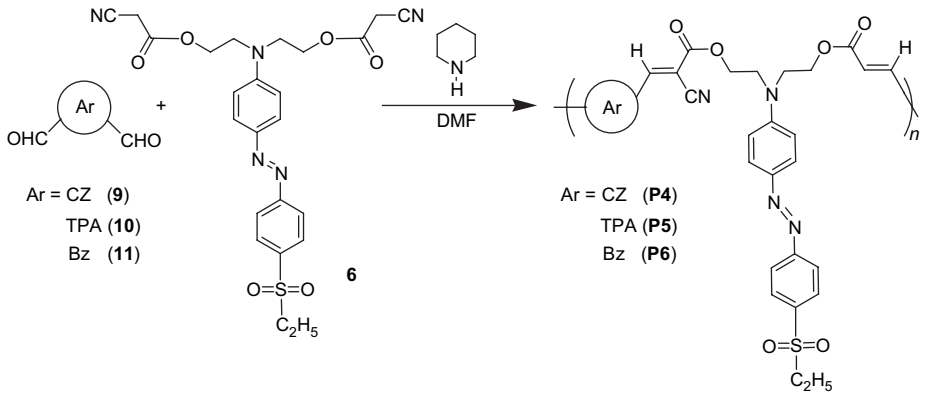

Scheme 3.

of the reaction mixtures into methanol from time to time, and stopped immediately when some solid precipitates appeared. Since the reactions proceeded in moderate rates, soluble products could be obtained. The products were purified by repeated precipitations of their THF solutions into methanol, and the purified products were obtained in good yields (Table 1). GPC analyses proved the polymeric nature of the products, although their M_w values seemed a little lower. However, it should be pointed out that the GPC analysis using linear polystyrenes as calibration standards often underestimates the molecular weights of hyperbranched polymers, with difference as big as ~40 times being reported in the literature [15]. The actual or true molecular weights of the *hb*-PAEs thus could be much higher than the values given in Table 1.

3.2. Structural characterization

All the compounds and polymers were well characterized, and the analytical data were shown in the Section 2. In the IR spectra of all the polymers, there is an apparently strong absorption band at 1129 cm^{-1}, which should be attributed to the characteristic peak of sulfonyl groups derived from the sulfonyl-based chromophore **6** or **7**. Also, the absorption bands at about 1720 and 2220 cm^{-1}, respectively, contributed by the carbonyl stretching vibration of a conjugated carboxylic ester and the nitrile stretching vibration, are easily found. The IR spectrum of **P1** is demonstrated in Fig. 1 as an example.

In all the ^1H NMR spectra of the polymers **P1**–**P6**, the chemical shifts are consistent with the proposed polymer structure as demonstrated in Schemes 2–3, and all the data are demonstrated in the Section 2. For example, Fig. 2 shows the spectra of **P1** and **P4**, it is obvious that the two curves are similar as their structure is alike. The signal of the proton in aldehyde groups at about 10 ppm, derived from the co-monomer **9**, nearly disappears in the spectrum of **P4**, and remains a little in **P1**, indicating the successful reaction between monomer **9** and chromophore **7** or **6**.

All the polymers, **P1**–**P5**, are easily soluble in polar solvents, such as DMF, DMSO, THF, etc., and **P6** exhibits similar solubility in solvents as others except THF. Fig. 3 shows the UV–vis spectra of them in the THF solutions, and the

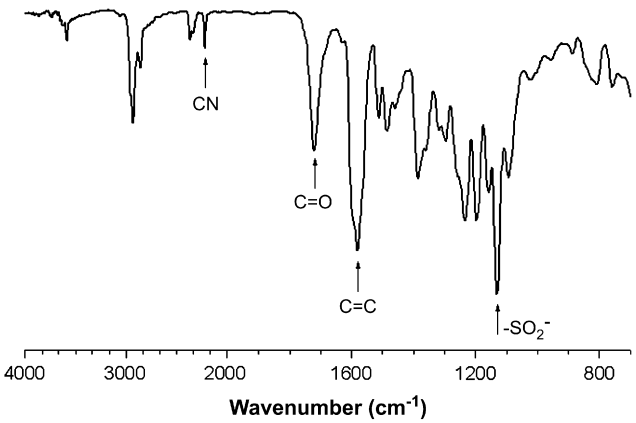

Fig. 1. IR spectra of **P1**.

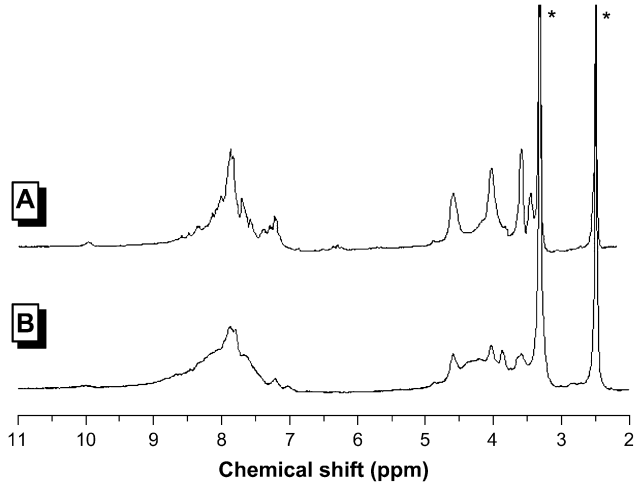

Fig. 2. ^1H NMR spectra of polymers in DMSO-d_6: (A) **P1**, (B) **P4**. The solvent peaks are marked with asterisks (*).

maximum data are summarized in Table 1 with those obtained from their solutions in DMF. It is easily seen that there are strong absorption peaks with the maximum absorption wavelengths longer than 400 nm and a band edge of ~550 nm, due to the π–π* transition of the sulfonyl-based chromophore. However, the maximum absorption wavelength of **P1** is blue-shifted more than 25 nm, compared with free chromophore molecules and other polymers with different co-monomers. Nearly the same maximum absorption wavelengths are observed in the case of **P4**. Even when the solvent is changed from THF to DMF, these two polymers still show much blue-shifted maximum absorption wavelengths. This is very interesting and would lead to even good transparency and reduced optical loss. In **P1**–**P6**, the chromophore moieties are surrounded by bulky phenyl rings derived from the co-monomer

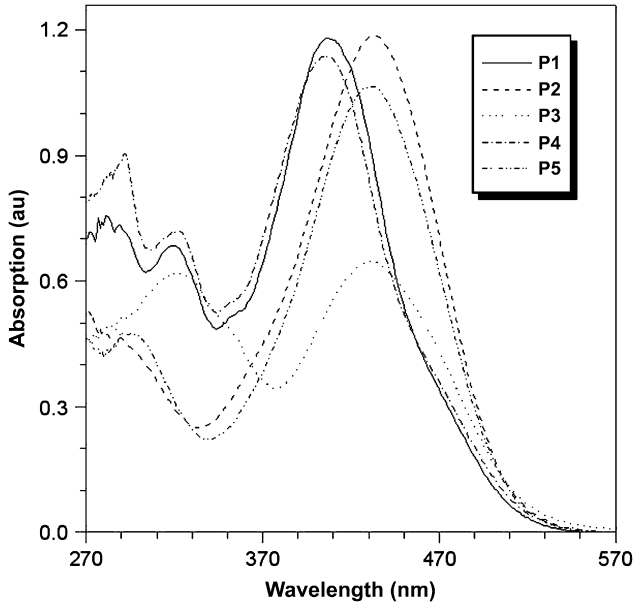

Fig. 3. UV–vis absorption spectra of THF solutions of polymers **P1**–**P5** (concentration: 0.02 mg/mL).

(**9** or **10** or **11**), thus it is possible to achieve effective site isolation, which would directly reduce the strong intermolecular dipole–dipole interactions between chromophore moieties and benefit the ordered noncentrosymmetric alignment during the poling process. And the site-isolation effect in **P1** and **P4**, indicated by the maximum absorption wavelengths in their UV–vis spectra, is more obvious than that in other polymers. Similar phenomena were reported in the literatures [5b,16].

The glass transition temperatures (T_g) of the polymers were measured by differential scanning calorimetry (DSC), and the results are summarized in Table 1. The moderate T_gs may be partially ascribed to the presence of bulky aromatic rings in the polymers, although the flexible alkyl spacer between the phenyl rings and chromophore moieties is a little longer. The polymers do not show any significant low temperature weight loss. The 5% weight loss temperatures are above 210 °C, and up to 271 °C (Table 1).

3.3. Nonlinear optical property

To evaluate the optical nonlinearity of **P1**–**P6**, their poled thin solid films are fabricated. Since **P3** and **P6** are easily crystallized to opaque solid state during the film fabrication process, their thin films could not be obtained by the process described in the Section 2. This might be due to their too high rigid structure. Thus, we tried to dope them in poly(methyl methacrylate) (PMMA), and got the thin films of **P3**, suitable for the NLO test, however, those of **P6** were not obtained.

The most convenient technique for measuring the second-order NLO activity is to investigate the SHG processes characterized by d_{33}. The d_{33} value for a poled film can be calculated from the equation given below [17]:

$$\frac{d_{33,s}}{d_{11,q}} = \sqrt{\frac{I_s}{I_q}}\frac{l_{c,q}}{l_s}F \tag{1}$$

where $d_{11,q}$ is the d_{11} of the quartz crystal (0.45 pm/V), I_s and I_q are the respective SHG intensities of the sample (polymer film) and the quartz crystal, $l_{c,q}$ is the coherent length of the quartz crystal, l_s is the thickness of the sample, and F is the correction factor of the apparatus (1.2 when $l_c \gg l_s$).

From the experimental data, the d_{33} values of the polymers are calculated, at the fundamental wavelength of 1064 nm (Table 1). Although various d_{33} values have been reported for different polymers containing similar azo dye moieties, and the d_{33} value of a NLO polymer can be different when measured by different methods or even by different testing systems, which makes direct data comparison difficult, it is still reasonable to compare the obtained results of **P1**–**P5** with each other and with the d_{33} values of the polymers carrying the similar sulfonyl-based chromophores calculated by the same method using the experimental data obtained from the same apparatus.

The linear polymers, **P4** and **P5**, show similar d_{33} values as other polymers containing nearly the same sulfonyl-based chromophores we reported previously [9]. It is exciting that the tested d_{33} values of the hyperbranched polymers, **P1** and **P2**, are much better than previous results, and up to 3.8 times higher than their corresponding linear analogues, which are prepared and tested at the same time. And **P3** also exhibits relatively high d_{33} value (20.6 pm/V), even tested in the doped PMMA film with the concentration only of 50% (w/w).

Generally, the concentrations of chromophore moieties in the polymer system would heavily influence the resultant NLO effect. According to the one-dimensional rigid orientation gas model [18]:

$$d_{33} = \frac{1}{2}N\beta f^{2\omega}(f^{\omega})^2\langle\cos^3\theta\rangle \tag{2}$$

where N is the number density of the chromophore, β is its first hyperpolarizability, f is the local field factor, 2ω is the double frequency of the laser, ω is its fundamental frequency, and $\langle\cos^3\theta\rangle$ is the average orientation factor of the poled film. Obviously, under identical experimental conditions, the d_{33} value is proportional to the number density of the chromophore moieties in the polymers. Thus, the real d_{33} value of **P3** should be much higher. And on the other hand, if we analyze the actual concentrations of the chromophore moieties in the polymers, it is obvious that the concentrations of the active sulfonyl-based chromophore moieties in hyperbranched polymers (**P1**–**P3**) are lower than those in their corresponding linear analogues (**P4**–**P5**). However, the d_{33} values of the hyperbranched polymers are much higher than those obtained for the linear polymers. Compared with other polymers with similar chromophore moieties we prepared previously [9,19], the d_{33} values of the hyperbranched polymers are still higher. However, most of the NLO polymers prepared so far possess linear molecular structures. The impressively higher d_{33} values of **P1**–**P3** suggest that the 3D architectural structure of the hyperbranched polymers and the spatial chromophore isolation in the macromolecular spheres have helped to enhance their optical nonlinearities, just as already shown in the NLO dendrimer systems. Unlike the NLO dendrimers and linear polymers containing dendronized chromophores, hyperbranched polymers are much easier

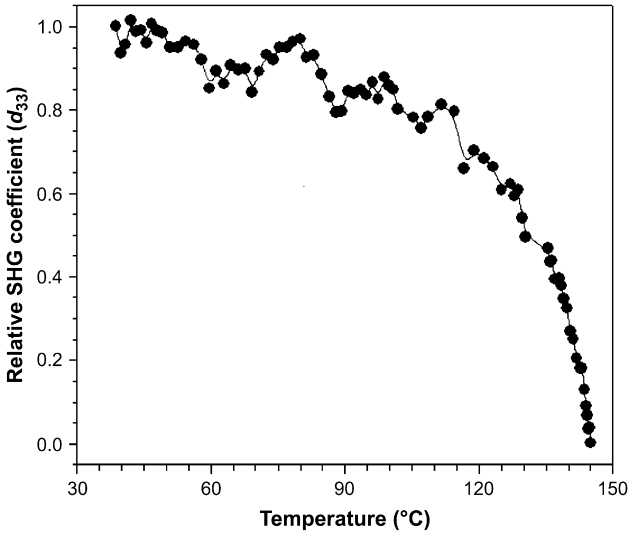

Fig. 4. Decays of SHG coefficients of **P2** as a function of temperature.

to be prepared from very flexible synthetic routes with convenient purification procedure.

The dynamic thermal stabilities of the NLO activities of the **P2** are investigated by depoling experiments for its highest T_g, in which the real time decays of their SHG signals are monitored as the poled films are heated from 45 to 150 °C in air at a rate of 4 °C/min. The onset temperature for decays in the d_{33} values is found to be 118 °C (Fig. 4), partially due to the high T_g value, because of their rigid molecular structures.

4. Conclusion

Through simple Knoevenagel reaction, three hyperbranched polymers (**P1**–**P3**) were successfully obtained, which contain the sulfonyl-based chromophore as the NLO active moieties. All the three hyperbranched polymers exhibit better NLO properties rather than their corresponding linear analogues, due to the three-dimensional spatial separation of the chromophores in them. Thus, hyperbranched NLO polymers might be another choice for us besides NLO dendrimers and polymers containing dendronized chromophores as side chains, to efficiently translate large molecular first hyperpolarizability (β) value of chromophores into high macroscopic second-harmonic generation (SHG) coefficient of materials.

Acknowledgements

We are grateful to the National Science Foundation of China (no. 20674059), the National Fundamental Key Research Program and Hubei Province for financial support.

References

[1] (a) Lee M, Katz HE, Erben C, Gill DM, Gopalan P, Heber JD, et al. Science 2002;298:1401;
(b) Shi Y, Zhang C, Zhang H, Bechtel JH, Dalton LR, Robinson BH, et al. Science 2000;288:119;
(c) Bai Y, Song N, Gao JP, Sun X, Wang X, Yu G, et al. J Am Chem Soc 2005;127:2060;
(d) Marder SR, Kippelen B, Jen AKY, Peyghambarian N. Nature 1997; 388:845.

[2] (a) Dalton LR, Robinson BH, Jen AKY, Steier WH, Nielsen R. Opt Mater 2003;21:19;
(b) Ma H, Jen AKY, Dalton LR. Adv Mater 2002;14:1339;
(c) Moerner WE, Jepsen AG, Thompson CL. Annu Rev Mater Sci 1997; 32:585.

[3] (a) Ma H, Jen AKY. Adv Mater 2001;13:1201;
(b) Wang Q, Wang LM, Yu LP. Macromol Rapid Commun 2000;21:723;
(c) Ma H, Liu S, Luo J, Suresh S, Liu L, Kang SH, et al. Adv Funct Mater 2002;12:565.

[4] (a) Robinson BH, Dalton LR. J Phys Chem A 2000;104:4785;
(b) Dalton LR, Steier WH, Robinson BH, Zhang C, Ren A, Garner S, et al. J Mater Chem 1999;9:19;
(c) Sullivan PA, Akelaitis AJP, Lee SK, McGrew G, Lee SK, Choi DH, et al. Chem Mater 2006;18:344.

[5] (a) Kim TD, Luo J, Tian Y, Ka JW, Tucker NM, Haller M, et al. Macromolecules 2006;39:1676;
(b) Luo JD, Ma H, Haller M, Jen AKY, Barto RR. Chem Commun 2002; 8:888;
(c) Haller M, Luo J, Li H, Kim TD, Liao Y, Robinson BH, et al. Macromolecules 2004;37:688.

[6] (a) Fréchet JMJ. Proc Natl Acad Sci USA 2002;99:4782;
(b) Hecht S, Fréchet JMJ. Angew Chem Int Ed 2001;40:74;
(c) Fréchet JMJ, Hawker CJ, Gitsov I, Leon JW. J Macromol Sci Pure Appl Chem 1996;A33:1399.

[7] (a) Czech P, Okrasa L, Méchin F, Boiteux G, Ulanski J. Polymer 2006; 47:7207;
(b) Sato T, Nakamura T, Seno M, Hirano T. Polymer 2006;47:4630;
(c) Ren Q, Gong F, Jiang B, Zhang D, Fang J, Guo F. Polymer 2006;47: 3382.

[8] (a) Jiang G, Wang L, Yu H, Chen C, Dong X, Chen T, et al. Polymer 2006;47:12;
(b) Zhou Z, Yan D. Polymer 2006;47:1473;
(c) Zhang J, Wang H, Li X. Polymer 2006;47:1511;
(d) Qin H, Mather PT, Baek JB, Tan LS. Polymer 2006;47:2813.

[9] (a) Li Z, Qin J, Li S, Ye C, Luo J, Cao Y. Macromolecules 2002;35:9232;
(b) Li Z, Huang C, Hua J, Qin J, Yang Z, Ye C. Macromolecules 2004;37: 371;
(c) Li Z, Qin A, Lam JWY, Dong Y, Dong Y, Ye C, et al. Macromolecules 2006;39:1436;
(d) Li Z, Li Z, Di C, Zhu Z, Li Q, Zeng Q, et al. Macromolecules 2006; 39:6951;
(e) Li Z, Li Q, Qin A, Dong Y, Lam JWY, Dong Y, et al. J Polym Sci Part A Polym Chem 2006;44:5672;
(f) Gong W, Li Q, Li Z, Lu C, Zhu J, Li S, et al. J Phys Chem B 2006; 110:10241.

[10] Courtin A. Helv Chim Acta 1983;66:1046.

[11] (a) Li Z, Qin J, Deng X, Cao Y. J Polym Sci Part A Polym Chem 2001; 39:3428;
(b) Li Z, Li J, Qin J. React Funct Polym 2001;48:113;
(c) Li Z, Luo J, Li J, Zhan C, Qin J. Polym Bull (Berlin) 2000;45:105.

[12] Broeck KV, Verbiest T, Degryse J, Beylen MV, Persoons A, Samyn C. Polymer 2001;42:3315.

[13] Cheuk KKL, Lam JWY, Lai LM, Dong Y, Tang BZ. Macromolecules 2003;36:9752.

[14] (a) Ulman A, Willand CS, Kohler W, Robello DR, Williams DJ, Handley L. J Am Chem Soc 1990;112:7083;
(b) Kohler W, Robello DR, Willand CS, Williams DJ. Macromolecules 1991;24:4589;
(c) Xu C, Wu B, Todorova O, Dalton LR, Shi Y, Ranon PM, et al. Macromolecules 1993;26:5303;
(d) Sohn J, Park SY, Moon H, Mun J, Yoon CS. React Funct Polym 2000; 45:109.

[15] (a) Muchtar Z, Schappacher M, Deffieux A. Macromolecules 2001;34: 7595;
(b) Weimer MW, Fréchet JMJ, Gitsov I. J Polym Sci Part A Polym Chem 1998;36:955;
(c) Kim Y, Webster OW. Macromolecules 1992;25:5561.

[16] Liao Y, Anderson CA, Sullivan PA, Akelaitis AJP, Robinson BH, Dalton LR. Chem Mater 2006;18:1062.

[17] Dalton LR, Xu C, Harper AW, Ghosn R, Wu B, Liang Z, et al. Mol Cryst Liq Cryst Sci Technol Sec B Nonlinear Opt 1995;10:383.

[18] Moylan CR, Miller RD, Twieg RJ, Lee VY, McComb IH, Ermer S, et al. Proc SPIE 1995;2527:150.

[19] (a) Li Z, Li J, Qin J, Qin A, Ye C. Polymer 2005;46:363;
(b) Li Z, Qin J, Li SJ, Ye C. Synth Met 2003;135:467;
(c) Li Z, Hua J, Li Q, Huang C, Qin A, Ye C, et al. Polymer 2005;46: 11940;
(d) Li Z, Gong W, Qin J, Yang Z, Ye C. Polymer 2005;46:4971.